15 December 2000

ELSEVIER

Chemical Physics Letters 332 (2000) 65–72

CHEMICAL PHYSICS LETTERS

www.elsevier.nl/locate/cplett

Photoelectron spectroscopy of clustered transition state precursors $IHI^- \cdot Ar$ and $BrHI^- \cdot Ar$

Zhuan Liu [a,b], Harry Gómez [a,b], Daniel M. Neumark [a,b,*]

[a] *Department of Chemistry, University of California, Berkeley, CA 94720, USA*
[b] *Chemical Sciences Division, Lawrence Berkeley National Laboratory, Berkeley, CA 94720, USA*

Received 11 September 2000; in final form 13 October 2000

Abstract

Photoelectron (PE) spectra of the $IHI^- \cdot Ar$ and $BrHI^- \cdot Ar$ clusters were measured in order to probe the effect of clustering on the transition state spectroscopy of the $X + HI \rightarrow XH + I$ (X = I, Br) reactions. Addition of one argon atom to XHI^- leads to a shift of the IHI^- and $BrHI^-$ spectra to lower electron kinetic energies by 18 and 36 meV, respectively. It also significantly reduces the contribution of vibrational hot bands to the photoelectron spectra. The $IHI^- \cdot Ar$ spectrum shows a new progression corresponding to hindered IHI rotor states near the $I + HI$ ($v = 1$) threshold. © 2000 Elsevier Science B.V. All rights reserved.

1. Introduction

Characterization of the transition state region of a chemical reaction is of fundamental importance in chemical reaction dynamics. In the past decades, there have been several experimental and theoretical studies on transition state spectroscopy and dynamics in the gas phase [1–5]. However, since most chemical reactions occur in solution, it is of interest to study the effect of solvation on chemical reaction dynamics. One way to address this issue is to probe the transition state region of a chemical reaction taking place in a size-selected cluster. Previously in this group, a powerful negative ion photodetachment technique has been developed to study the transition state spectroscopy of bimolecular gas phase reactions [6,7]. In the present Letter, we extend this technique to explore the effect of clustering on transition state spectroscopy and dynamics. As a first step we present the result on the bimolecular reactions $X + HI \rightarrow XH + I$ (X = Br and I) in argon clusters by measuring the photoelectron spectra of $IHI^- \cdot Ar$ and $BrHI^- \cdot Ar$.

The transition state spectrum of the $I + HI$ reaction, obtained by photoelectron spectroscopy of the IHI^- anion, was first reported by Weaver et al. [8]. A well-resolved progression in the antisymmetric (H-atom) stretch vibration of the neutral IHI complex was observed. A higher resolution study of IHI^- by Waller et al. [9] using anion zero electron kinetic energy (ZEKE) spectroscopy revealed more underlying structure in each of the three peaks observed by Weaver et al. [8]. In particular, progressions in the much lower frequency symmetric (I-atom) stretch were resolved; these are associated with reactive resonances in the

* Corresponding author. Fax: +1-510-642-6262.
E-mail address: dan@radon.cchem.berkeley.edu (D.M. Neumark).

PII: S0009-2614(00)01243-4

transition state. The ZEKE spectrum also showed transitions to hindered rotor states of the neutral IHI complex. The transition state region of the Br + HI reaction was probed by photoelectron spectroscopy of $BrHI^-$ as reported by Bradforth et al. [10]. The observed spectrum was similar to that of IHI^-, in that too it was dominated by a progression in the asymmetric stretch motion of the dissociating BrHI complex. However, the peaks were considerably broader and more uniform in width in the $BrHI^-$ spectrum.

Transition state spectroscopy experiments on clustered IHI^-, specifically $IHI^-(N_2O)_n$ clusters, were reported by Arnold et al. [11,12]. In these spectra, the overall features resembled those observed for bare IHI^- but were shifted to lower electron kinetic energies due to the effect of solvation. In addition, the spacing of the antisymmetric stretch progression was different in $IDI^-(N_2O)$ compared to bare IDI^-. This result was explained by postulating a small change in anion geometry resulting from the interaction between the anion and solvating species, shifting the Franck–Condon (FC) region to a larger I–I distance with an accompanying change in the neutral vibrational level spacing.

In this Letter, the photoelectron spectra of $XHI^- \cdot Ar(X = Br, I)$ are reported; results for larger clusters will be covered in a subsequent publication. Compared to N_2O, Ar atoms should interact more weakly with the anion and neutral species. Nonetheless, clusters with Ar are of considerable interest for two reasons. First, calculations of the photoelectron spectra of $ClHCl^-(Ar)_n$ clusters have been carried out by McCoy and coworkers [13], thereby offering an opportunity to make detailed comparisons between experiment and theory. In addition, anion infrared and photoelectron spectroscopy measurements have shown that spectral congestion and other effects from vibrationally hot anions can be greatly reduced through complexation of argon atoms to negative ions [14,15]. This cooling occurs because those negative ions for which the vibrational excitation energy exceeds the binding energy of the argon atom undergo predissociation, reducing the contribution of vibrational hot bands to the photoelectron spectrum. We indeed find that clustering of a single argon atom to bihalide ions dramatically cleans up the photoelectron spectra of IHI^- and $BrHI^-$ and, for the former, reveals new transition state resonances and rotational threshold transitions that were previously obscured by spectral congestion. The spectra also provide new information on the clustering energetics of both species.

2. Experimental

The negative ion time-of-flight (TOF) photoelectron spectrometer used in this Letter has been described in detail previously [16,17], and only particulars relevant to the present results are given here. Anion clusters are produced at the intersection of a pulsed molecular beam and a 1 keV, 300 μÅ electron beam. The molecular beam is formed from a gas mixture of 0.1% HI (for $IHI^- \cdot Ar$) or 0.05% HI, 0.1% HBr (for $BrHI^- \cdot Ar$) in argon carrier gas which is expanded through a piezoelectric valve (0.1 mm diameter orifice) operated at 20 Hz with a stagnation pressure of 40 psi. Anion clusters generated in the supersonic expansion are cooled internally and extracted perpendicularly to the expansion by a pulsed electric field. They are then accelerated to a beam energy of 2.5 keV and enter a linear reflectron TOF mass spectrometer. The extracted ions separate in time and space according to their mass-to-charge ratios and are detected at the end of the flight tube by a pair of 25 mm diameter chevron-mounted microchannel plates.

Photoelectrons are detached from the mass-selected ions by a laser pulse from a Nd:YAG laser operated at 20 Hz. The ion of interest is selectively photodetached by controlling the laser firing delay. In the present Letter, the fourth harmonic (266 nm, 4.66 eV) of the Nd:YAG laser is used. Photoelectron energies are determined by TOF measurements in a 1 m field-free flight tube. In all experiments reported here, the laser beam is plane polarized perpendicular to the direction of electron collection. The resolution of the apparatus is 8–10 meV for an electron kinetic energy (eKE) of 0.65 eV and degrades as $(eKE)^{3/2}$ at higher eKEs. The 266 nm photons generate a very small background

signals through the interaction of scattered light with metal surfaces. A background spectrum, collected using the same laser power used during data collection, is fitted to a smooth function which is scaled and subtracted from the acquired data. The measured spectra are calibrated using the known photoelectron spectra of I^-, Cl^- and Br^-.

3. Results

The photoelectron (PE) spectra of $IHI^- \cdot Ar$ and $BrHI^- \cdot Ar$ collected are shown in Fig. 1 together with the PE spectra of IHI^- and $BrHI^-$. In previous work [8], the main progression in the IHI^- PE spectrum (A, B, C) was assigned to transitions to antisymmetric (ν_3) stretch levels of the IHI complex, specifically the $\nu_3' = 0, 2$, and 4 levels (ν_n' and ν_n'' refer to neutral and anion vibrational levels, respectively). The progression a, b, c in $BrHI^-$ results from the same vibrational motion (ν_3) but with a somewhat different vibrational assignment ($\nu_3' = 0, 1$ and 3) [10]. The spectra of $IHI^- \cdot Ar$ and $BrHI^- \cdot Ar$ are, at first glance, quite similar to those of the bare ions, with no observable change in the peak spacing for the major features associated with the ν_3 progressions. However, there are clear differences between the two sets of spectra.

First, addition of one argon atom to IHI^- and $BrHI^-$ leads to shifts of the spectra towards lower eKE. The spectral shifts of $IHI^- \cdot Ar$ and $BrHI^- \cdot Ar$ compared to IHI^- and $BrHI^-$ are 18 and 36 meV (using peaks (B, B') and (a, a')), respectively. Another significant effect due to argon clustering is the change of the peak shapes. For example, the long extended wing on the high eKE side of the $\nu_3' = 0$ features of IHI^- disappears in the cluster PE spectrum, and the onset of signal occurs at a much lower eKE of 0.79 eV, with a similar effect seen for $BrHI^-$. More generally, the linewidths of the spectra of $IHI^- \cdot Ar$ and $BrHI^- \cdot Ar$ are noticeably narrower compared to that of the corresponding features of bare XHI^- anions.

A more subtle result due to argon clustering is the observation of some small features in the $IHI^- \cdot Ar$ spectrum. These are shown in more detail in Fig. 2, along with the high resolution ZEKE spectrum of IHI^-, the latter shifted by 18 meV for comparison. In the $IHI^- \cdot Ar$ spectrum, six small peaks (a, b, c, d, e, f) are superimposed on the overall $\nu_3' = 0$ feature, forming a progression with peak intervals of approximately 160–210 cm^{-1}.

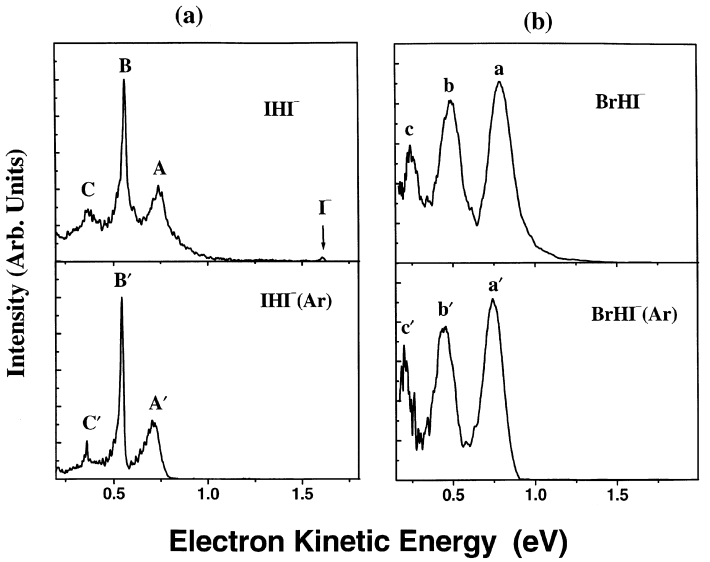

Fig. 1. Comparison between the PE spectra of bare (XHI^-) and argon clustered anions ($XHI^- \cdot Ar$) at 266 nm: (a) IHI^- and $IHI^- \cdot Ar$; (b) $BrHI^-$ and $BrHI^- \cdot Ar$.

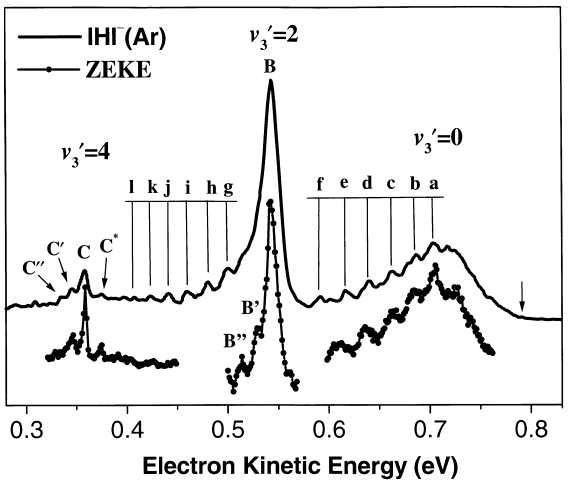

Fig. 2. Expanded view of the photoelectron spectrum of $IHI^- \cdot Ar$, plotted together with the ZEKE spectrum of IHI^-. The ZEKE spectrum is shifted to lower electron kinetic energy by 18 meV.

Another weak progression (g, h, i, j, k, l) is seen starting at an electron kinetic energy of ~0.5 eV, about 53 meV lower than the $v_3' = 2$ peak, B. These peaks are separated by intervals of ~150–190 cm^{-1}, similar to the $v_3' = 0$ progression and with very similar linewidths (~60–80 cm^{-1}). Finally, we resolve four peaks associated with the $v_3' = 4$ feature. Peaks C, C′ and C″ form a progression with a spacing of about 100 cm^{-1}. Peak C^* is about 130 cm^{-1} higher in electron kinetic energy than peak C. Comparison with the ZEKE spectrum shows a close correspondence between the fine structure associated with the $v_3' = 0$ and 4 peaks, but the peaks (g, h, i, j, k, l) in the PE spectrum are new features that occur in a spectral region not scanned in the ZEKE spectrum. Table 1 lists the positions of all observed peaks in the $IHI^- \cdot Ar$ spectrum.

Table 1
Peak positions (eV) of the PE spectrum of $IHI^- \cdot Ar$ at 266 nm

$v_3' = 0$		$v_3' = 2$		$v_3' = 4$	
a	0.712	B	0.539	C	0.345
b	0.693	g	0.492	C′	0.332
c	0.666	h	0.473	C″	0.31
d	0.642	i	0.456	C^*	0.361
e	0.622	j	0.434		
f	0.595	k	0.410		
		l	0.390		

We have also examined the $BrHI^- \cdot Ar$ spectrum carefully for additional structure. Apart from the three main peaks mentioned above, there are two weak peaks around 0.6 eV, near the trough between peaks a′ and b′.

4. Discussion

In this section, the differences between the PE spectra of the bare and clustered anions in Fig. 1 are considered in more detail. We first consider the spectral shifts between the two sets of spectra. This effect, seen in many other photoelectron spectra [14,18–20], results from stronger binding of the Ar atom to the anion than to the neutral. Ar atoms bind to the $IHI^-/BrHI^-$ anion, through the charge-induced dipole interaction, whereas binding to the neutral complex is from the much weaker van der Waals interaction. As a consequence, addition of an argon atom to the anion will stabilize the anion more than the neutral complex, leading to a shift of the photoelectron spectrum towards lower electron kinetic energy.

Using the spectral shifts observed in the PE spectra, we can estimate the bond dissociation energies of the $IHI^- \cdot Ar$ and $BrHI^- \cdot Ar$ clusters. The bond dissociation energy of $HI^- \cdot Ar$ can be determined by

$$D_0(XHI^- \cdots Ar) = \Delta SE + D_0(XHI \cdots Ar), \qquad (1)$$

where ΔSE is the shift of the PE spectrum, which corresponds to the difference of solvation energies between anion and neutral clusters. $D_0(XHI \cdot Ar)$ is the binding energy of the neutral $XHI \cdot Ar$ complex. This is not a well-defined parameter as XHI is not a stable molecule. However, it is reasonable to define $D_0(XHI \cdot Ar)$ as the binding energy of the Ar atom to the XHI complex in the geometry accessed by vertical photodetachment from the anion. We then approximate $D_0(XHI \cdot Ar)$ as the sum of the van der Waals interaction energies of $X \cdot Ar$ and $I \cdot Ar$, assuming that the Ar atom forms a T-shaped complex with the two halogen atoms in $XHI^- \cdot Ar$ clusters (as it does in $I_2^- \cdot Ar$ [14]). Using $D_0(I \cdot Ar) = 128 \pm 18$ cm^{-1} and $D_0(Br \cdot Ar) = 111 \pm 8$ cm^{-1} [18], we have $D_0(IHI \cdot Ar) \sim 256$ cm^{-1} and $D_0(BrHI \cdot Ar)$

~ 239 cm^{-1}. The dissociation energies of $IHI^- \cdot Ar$ and $BrHI^- \cdot Ar$ are then about 400 and 530 cm^{-1}, respectively. $D_0(IHI^- \cdot Ar)$ is close to $D_0(I^- \cdot Ar) = 370 \pm 18$ cm^{-1} [18] and $D_0(I_2^- \cdot Ar) = 427 \pm 32$ cm^{-1} [14], while $D_0(BrHI^- \cdot Ar)$ is slightly larger than $D_0(I^- \cdot Ar)$ and $D_0(Br^- \cdot Ar) = 435 \pm 8$ cm^{-1} [18].

In the PE spectrum of the $I_2^- \cdot Ar$ cluster reported by Asmis et al. [14], a prominent vibrational cooling effect due to evaporative cooling was observed. Related effects have been observed by Johnson and co-workers [15] in the infrared spectra of $X^-(H_2O)_n$ ions. Evaporative cooling is also clearly demonstrated in our results in Fig. 1 where the long wings towards high eKE in the IHI^- and $BrHI^-$ spectra disappear in the corresponding $XHI^- \cdot Ar$ spectra. For $IHI^- \cdot Ar$, the bond dissociation energy obtained above is about 400 cm^{-1}, which lies above the symmetric stretch (ν_1) frequency (130 cm^{-1}) [21] and below the antisymmetric (ν_3) and bending (ν_2) frequencies 672 cm^{-1} [21] and $\sim$700 cm^{-1} [22], respectively). A similar situation holds for $BrHI^- \cdot Ar$ [22,23]. Hence, excitation of even one quantum of the relatively high frequency H-atom vibrational modes in either ion should result in predissociation of the $XHI^- \cdot Ar$ complex during the time interval of several hundred μs between ion formation and mass separation in the reflectron, so that the only $XHI^- \cdot Ar$ that survive are those in which the XHI^- moiety has at the most a few quanta of symmetric stretch excitation.

The disappearance of the high eKE 'tails' in the $XHI^- \cdot Ar$ spectra shows definitively that they are from vibrationally excited anions, thus resolving an issue that was unclear when the bihalide PE spectra were first published [8]. The observations of considerably more fine structure in the $IHI^- \cdot Ar$ spectrum and the narrowing of the peaks in the $BrHI^- \cdot Ar$ spectra in comparison to the bare anion PE spectra are also attributed to the reduction of spectral congestion through evaporative cooling; both of these features are worthy of further discussion.

Fig. 2 shows that the finer structure associated with the $v_3' = 0$ and 4 in the $IHI^- \cdot Ar$ spectrum matches that seen in the higher resolution IHI^- ZEKE spectrum, so the features in the two spectra presumably have the same origin. Note that the ZEKE spectrum of IHI^- appears free of the spectral congestion seen in the bare IHI^- PE spectrum, implying that colder anions are produced in the ZEKE spectrometer. Based on the assignment of the ZEKE spectrum by Waller et al. [9], the progression in the $v_3' = 0$ peak of $IHI^- \cdot Ar$ is attributed to photodetachment transitions to internal rotor states of the IHI complex. The progression C, C′ and C″ in the $v_3' = 4$ group in the ZEKE spectrum was assigned to quasi-bound reactive resonances associated with the symmetric stretch of the IHI complex, while peak C* is a hot band transition originating from the $v_1'' = 1$ symmetric stretch level of the anion; these assignments also apply to the $IHI^- \cdot Ar$ PE spectrum.

The distinction between the two types of states of the IHI complex can be understood with reference to Fig. 3, which shows three-dimensional adiabatic curves derived by Metz and Neumark [22] for a model I + HI potential energy surface, the LEPS-C surface developed by Schatz et al. [24]. These curves, as originally described by Kubach et al. [25], show how I + HI (v, j) levels evolve adiabatically as the two I atoms are brought together and are obtained by solving the two-dimensional Schrodinger equation for H-atom stretching and bending motion at fixed I–I bond distance. Only vibrational levels with *gerade*

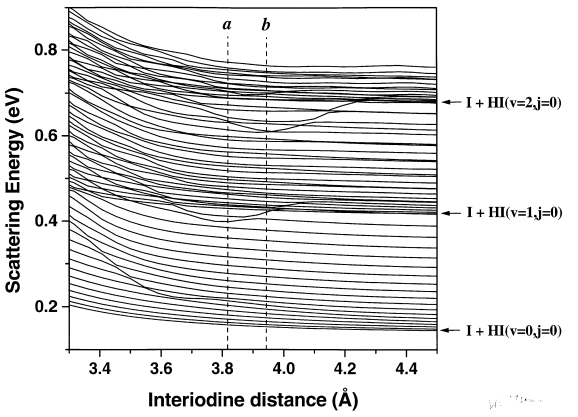

Fig. 3. Three-dimensional adiabatic curves calculated by Metz and Neumark [22] for the I + HI reaction on the LEPS-C potential. The FC region for photodetachment is indicated by two vertical lines, a and b.

symmetry are shown, i.e., even v_3 levels, since transitions to odd v_3 levels of the complex from the anion ground state are forbidden. Hence, asymptotic $I + HI$ $(v = n)$ levels correlate to IHI $(v_3 = 2n)$ levels. The vertical lines a and b in Fig. 3 represent the FC region for photodetachment, i.e., the inner and outer turning points of the IHI^- ground state wavefunction. The adiabatic curves correlating to $I + HI(v = 0, j)$, i.e., those associated with transitions to the IHI $(v_3' = 0)$ feature, are repulsive in the FC region; transitions to these curves are responsible for the hindered rotor progression. On the other hand, adiabatic curves near the $I + HI$ $(v = 2, j = 0)$ asymptote have wells in the FC region, resulting in a progression in the quasi-bound symmetric stretch vibration associated with the $v_3' = 4$ feature [26].

We now consider the more extensive structure associated with the $v_3 = 2$ feature. In the ZEKE spectrum, a progression B, B′ and B″ spaced by $\sim$100 cm^{-1} is partially resolved. These peaks were previously assigned to reactive resonances with shorter lifetimes than those associated with the $v_3' = 4$ feature. These three peaks are not as well resolved in the $IHI^- \cdot Ar$ PE spectrum, with B′ and B″ possibly appearing as shoulders on the main feature B, presumably because of the lower spectral resolution of the PE spectrometer. However, the PE spectrum shows an additional progression (g, h, i, j, k, l) at slightly lower eKE than peak B. This progression has peak intervals of about 150–190 cm^{-1}, significantly different from the B, B′ and B″ progression. So these peaks are not simply the extension of the symmetric stretch progression. Instead, their spacing is characteristic of the internal rotor progression associated with the $v_3' = 0$ feature, and we therefore assign peaks $g - l$ to a progression of internal rotor states of the IHI complex correlating to $I + HI$ $(v = 1, j)$.

Thus, it appears the $v_3' = 2$ feature is associated with two progressions, one due to resonance features and the other to internal rotor states. This intermediate behavior can be understood with reference to the adiabatic curves near the $I + HI$ $(v = 1, j = 0)$ asymptote (Fig. 3); the FC region includes a shallow well that supports quasi-bound states as well as repulsive adiabatic curves at higher energy leading to a progression in internal rotor states of the complex. We note that simulations by Metz and Neumark [22] of the IHI^- photoelectron spectrum using the adiabatic curves of Fig. 3 yielded qualitative agreement with many of the experimental results, including the observation of resonances and internal rotor progressions associated with the $v_3' = 2$ feature.

We close by considering the $BrHI^- \cdot Ar$ spectrum in more detail. The FC region for $BrHI^-$ photodetachment lies on the $I + HBr$ product side of the reaction coordinate [10], and no transition state resonances are expected in the PE spectrum. In a previous simulation of the PE spectrum of $BrHI^-$ by Metz and Neumark [22] using the three-dimensional adiabatic method and the Broida–Persky LEPS surface [27] for the $Br + HI$ reaction, the peak positions of the $v_3' = 0$ and 1 features in the $BrHI^-$ PE spectrum were reproduced. However, the peak widths in the simulations of 100 and 85 meV, respectively, for these features were considerably narrower than the experimental peak widths of 160–170 meV [10]. This discrepancy was attributed to possible inaccuracies in the model $Br + HI$ surface. In Fig. 4, the simulated spectrum by Metz et al. is plotted together with our $BrHI^- \cdot Ar$ spectrum, with the simulated spectrum shifted to lower eKE by 110 meV. These two spectra agree reasonably well in both peak posi-

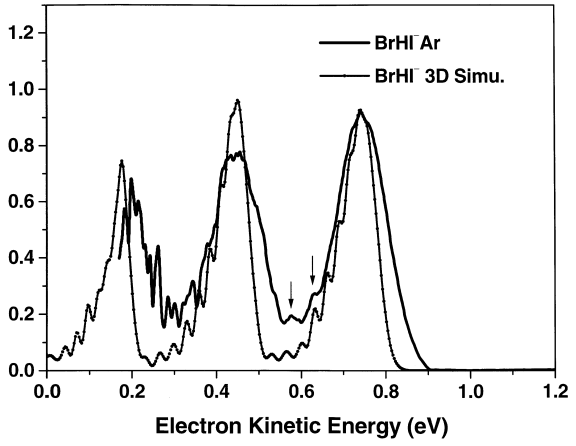

Fig. 4. The photoelectron spectrum of $BrHI^- \cdot Ar$ plotted together with the simulated PE spectrum of $BrHI^-$ by Metz and Neumark [22] using the three-dimensional adiabatic method. The simulated spectrum is shifted to lower eKE by 110 meV.

tions and widths. The experimental peak widths of ~130 meV are only slightly larger than the simulation, showing that the previous discrepancy was mainly due to anion hot bands. In the three-dimensional adiabatic simulation, the spectrum shows some partially resolved structure due to rotational thresholds. This structure is not clearly resolved in the experimental spectrum; only some weak features, indicated by arrows in Fig. 4, were observed. A higher resolution spectrum using ZEKE could possibly resolve this structure, which would provide important information on the Br + HI potential energy surface.

5. Summary

In this Letter, we have investigated the photoelectron spectra of the clustered transition state precursors $IHI^- \cdot Ar$ and $BrHI^- \cdot Ar$ as a first step towards understanding how clustering effects transition state spectroscopy and dynamics. Clustering with a single argon atom results in two notable effects. First, the overall features of the transition state spectra are shifted to lower eKE. Second, the contribution of vibrational hot bands to the spectra is significantly reduced, giving much better spectral resolution. This improvement allows us to observe reactive resonances and transitions to hindered rotor states for the I + HI reaction. A new progression due to IHI hindered rotor states near the I + HI $(v = 1)$ scattering channel was observed. Appearance of this progression together with the symmetric stretch vibration in the $v_3' = 2$ level indicates that the photodetachment process accesses both resonance and direct scattering wavefunctions of the I + HI reaction. Clustering also reduces the widths of the peaks in the $BrHI^-$ PE spectrum, bringing them into much better agreement with earlier simulations using a model Br + HI potential energy surface.

In the future, we plan to measure the PE spectra of other bihalide anions in argon clusters, e.g., $ClHCl^- \cdot Ar$, $BrHBr^- \cdot Ar$, etc. Experimental evidence of reactive resonances in the corresponding Cl + HCl and Br + HBr reactions is far less definitive than for I + HI. The PE spectra of $ClHCl^- \cdot Ar$ and $BrHBr^- \cdot Ar$ may reveal new structures associated with the transition state dynamics which were not observed in the PE spectra of the bare ions [16].

Acknowledgements

This research is supported by Air Force Office of Scientific Research under Grant No. F49620-00-1-0145.

References

[1] A.H. Zewail, Science 242 (1988) 1645.
[2] P.R. Brooks, Chem. Rev. 88 (1988) 407.
[3] G.C. Schatz, J. Phys. Chem. 94 (1990) 6157.
[4] D.M. Neumark, Annu. Rev. Phys. Chem. 43 (1992) 153.
[5] J.C. Polanyi, A.H. Zewail, Acc. Chem. Res. 28 (1995) 119.
[6] R.B. Metz, S.E. Bradforth, D.M. Neumark, in: I. Prigogine, S.A. Rice (Eds.), Advances in Chemical Physics, vol. 91, Wiley, New York, 1992.
[7] D.M. Neumark, Acc. Chem. Res. 26 (1993) 33.
[8] A. Weaver, R.B. Metz, S.E. Bradforth, D.M. Neumark, J. Phys. Chem. 92 (1988) 5558.
[9] I.M. Waller, T.N. Kitsopoulos, D.M. Neumark, J. Phys. Chem. 94 (1990) 2240.
[10] S.E. Bradforth, A. Weaver, D.W. Arnold, R.B. Metz, D.M. Neumark, J. Chem. Phys. 92 (1990) 7205.
[11] D.W. Arnold, University of California, Berkeley, CA, 1994 (Chapter 9).
[12] D. M. Neumark, in: J.M. Brauman, M.A. Ratner (Eds.), Advances in Molecular Vibrations and Collision Dynamics, vol. 1A, JAI Press, Greenwich, CT, 1991.
[13] H.B. Lavender, A.B. McCoy, J. Phys. Chem. A 104 (2000) 644.
[14] K.R. Asmis, T.R. Taylor, C.S. Xu, D.M. Neumark, J. Chem. Phys. 109 (1998) 4389.
[15] P. Ayotte, G.H. Weddle, J. Kim, M.A. Johnson, Chem. Phys. 239 (1998) 485.
[16] R.B. Metz, A. Weaver, S.E. Bradforth, T.N. Kitsopoulos, D.M. Neumark, J. Phys. Chem. 94 (1990) 1377.
[17] C. Xu, G.R. Burton, T.R. Taylor, D.M. Neumark, J. Chem. Phys. 107 (1997) 3428.
[18] Y.X. Zhao, I. Yourshaw, G. Reiser, C.C. Arnold, D.M. Neumark, J. Chem. Phys. 101 (1994) 6538.
[19] G. Markovich, R. Giniger, M. Levin, O. Cheshnovsky, J. Chem. Phys. 95 (1991) 9416.
[20] S.T. Arnold, J.H. Hendricks, K.H. Bowen, J. Chem. Phys. 102 (1995) 39.
[21] D.L. Lugez, M.E. Jacox, W.E. Thompson, J. Chem. Phys. 105 (1996) 3901.
[22] R.B. Metz, D.M. Neumark, J. Chem. Phys. 97 (1992) 962.

[23] C.M. Ellison, B.S. Ault, J. Chem. Phys. 83 (1979) 832.
[24] G.C. Schatz, D. Sokolovski, J.N.L. Connor, Discuss. Faraday Soc. (1991) 17.
[25] C. Kubach, G.N. Vien, M. Richardviard, J. Chem. Phys. 94 (1991) 1929.
[26] G.N. Vien, N. Rougeau, C. Kubach, Chem. Phys. Lett. 215 (1993) 35.
[27] M. Broida, A. Persky, Chem. Phys. 133 (1989) 405.